ISSN : 0974 - 7435 Volume 10 Issue 24

2014

BioTechnology

An Indian Journal

FULL PAPER

BTAIJ, 10(24), 2014 [15082-15094]

Optimal operation of active distribution systems for maximizing renewable energy usage

Xu Yang, Jianhua Zhang*

Department of Electrical and Electronic Engineering, North China Electric Power University, Changping District, 102206, Beijing, (CHINA)

E-mail : dongjunncepu@126.com

ABSTRACT

The planning methods and operation modes of traditional distribution network are difficult to accommodate the high penetration of distributed energy resources (DERs). Active distribution network (ADN), based on the application of information and communication technology (ICT) and advanced metering infrastructure (AMI), is one of the alternative solutions. This paper proposes a multi-objective optimization method for ADN operation. Analyzing the DG active/reactive power decoupling control ability under the inverter-based interface mode and putting forward an ADN cross-regional energy utilization strategy, a ADN multi-objective optimization dispatching model is established aiming at the minimum of system operation costs, DREG curtailment and the network loss. It is solved with MOHS algorithm. The optimizing model is able to realize comprehensive benefit of ADN operation on the premise of prior utilization of renewable energy. It is suitable for multiple system operators and the relevant results could offer theoretical foundation and experience to the formulation of ADN operation dispatching strategy.

KEYWORDS

Active distribution network; Renewable energy; Operation optimization; Multi-objective harmony search algorithm.

INTRODUCTION

Due to the global environment crisis and the continuing decrease of the conventional fossil energy, the Distributed Renewable Energy Generation (DREG) shares a rapid development. With the large-scale of the DREG (e.g. wind power, photovoltaic power) connecting to various voltage network, the significant challenge of distribution network management is how to maximize the utilization of the renewable energy while ensuring safe and economical operation of the power grid [1].

As an important form of the smart grid, ADN is an effective technology to realize the target above. Different from the user-oriented microgrid technology, ADN is duty of implementing comprehensive coordinated management to all kinds of distributed resources (including Distributed Generation (DG), Energy Storage System (ESS), Interruptible Loads (IL), etc.) [2, 3]. Therefore, ADN has the distinctive characteristics not only in the mode of operation but also in the control objectives. And under the influence of the various DER and their control methods, ADN is complicated to operate considering the control dimensions and the optimization space, which also makes higher request for the properties of the algorithm.

There have been many relevant researches for the operational control of ADN. Ref. [4] built an ADN optimal dispatch model that is oriented to the active control of the wind power based on the communication standards IEC. To minimize the cost of system operation, Refs. [5-7] built a day-ahead/intra-day ADN optimal dispatch model applying the Optimal Power Flow (OPF) technique. On the basis, Ref. [8] analyzed the influence of price fluctuation, switch action and scheduling sequence of DGs on the operation cost under ADN framework. Ref. [9] emphasized on the temporal section coupling character of ESS and controllable loads (CLs). Aiming at the minimization of power from upper grid, a dynamic scheduling model is proposed. Considering particular constraints is not to be satisfied all the time in the actual operation, Ref. [10] came up with an ADN energy dispatching strategy based on the chance constrained programming. Under the idea of decentralized control and centralized optimization, Ref. [11] established an ADN OPF model in multiple time scales, realizing DG coordinated control. Few optimization of the active power is still far from achieving global optimization in the ADN owing to the coupling relationship between the active and reactive power. For this reason, Ref. [12] used mixed integer second-order cone programming and presented an ADN optimizing operation model as well as its fast solving strategy considering the coordinated control of DG and reactive power control devices.

The achievements above settled a significant foundation for the researches in this field, but there are still deficiencies in three aspects: 1) Regarding model optimization, existing researches have not adequately analyzed or applied the true characteristics of ADN. Most of the models only considered factors such as system operating costs and network loss, without precisely reflecting the objectives of ADN to promote the active utilization of clean energy. 2) Regarding modeling approaches, as for the multiple targets of ADN operation, the majority of the researches simply used weighted summation to transfer the problems into single-target ones. This method is probably to lead to large deviation between the strategy and the operator's subjective because it is difficult to represent explicitly the inter links between different properties. 3) Regarding control objects, present researches mostly disposed DREG as un-dispatching units based on maximum power point tracking, neglecting the flexible reactive power regulating ability of DREG and its influence on ADN operation. Therefore, it is difficult to ensure that the dispatching scheme possesses global optimization.

Focusing on the problems above, this paper proposes a multi-objective optimization framework for ADN operation which promotes cross-regional utilization of renewable energy. Based on the analysis of the active/reactive power regulating ability of DG under decoupling method, the strategy for ADN operation considering cross-regional usage of renewable energy is put forward, and a multi-objective day-ahead optimal dispatch model is built. The active/reactive power output of DGs, ESS and ILs has been considered in this model with inter-temporal constraints of DER taken into account. The proposed model is effectively solved by the Multi-objective Harmony Search (MOHS) algorithm and the effectiveness is verified on relevant results.

THE DG ACTIVE/REACTIVE DECOUPLING CONTROL MODEL BASED ON INVERTER INERFACE

Under ADN, due to the implementation of the Active Network Management (ANM) mode, all kinds of DG transfer from "invisible" sources in conventional distribution network to controllable units that can be deeply involved in system's overall energy dispatch. Because of the fluctuation of renewable energy, there are two basic modes of DREG control: non-control and the power factor control [1]. In the non-control mode, all the energy from DREGs is not controlled, and the Distribution Management System (DMS) controls other schedulable units (e.g. micro gas turbines, ESS, CLs, etc.) to realize the optimal operation of the system. Since DREG operate as uncontrollable units, it is difficult to deal with the problems of voltage deviation and transmission congestion caused by the high permeability of DREG. In the power factor control mode, DMS actively controls DREG by regulating the power factor. However, the reactive output of DG is also influenced by the fluctuation of its active power due to their coupling relationship. Therefore the flexibility of this mode is not able to meet the objective of ADN optimal operation. In view of these shortages, this paper analyzes the strategy of DG active/reactive decoupling control based on inverter interface model [13-14].

Figure 1 is the schematic diagram of DG control system under inverter interface model. In the synchronization pattern, the derivation of the DG active/reactive decoupling control ability is as follows: Considering the converter output current of DG I_c remains in certain conditions, the relationship of the port active, reactive power and the voltage can be expressed as:

$$P_{\mathrm{DG}}^2 + Q_{\mathrm{DG}}^2 = \left(V_{\mathrm{g}} I_{\mathrm{c}}\right)^2 \tag{1}$$

$$P_{\mathrm{DG}}^2 + \left(Q_{\mathrm{DG}} + I_{\mathrm{c}}^2 X_{\mathrm{c}}\right)^2 = \left(V_{\mathrm{c}} I_{\mathrm{c}}\right)^2 \tag{2}$$

where X_c is the resistance value of the overall transformers and filters from the DG exit to the synchronization point. Formula (2) can be rewritten as:

$$P_{\mathrm{DG}}^2 + \left(Q_{\mathrm{DG}} + \frac{V_{\mathrm{g}}^2}{X_{\mathrm{c}}}\right)^2 = \left(\frac{V_{\mathrm{c}} V_{\mathrm{g}}}{X_{\mathrm{c}}}\right)^2 \tag{3}$$

Combining (2) and (3), we can understand that when the value of the active power is certain, DG output reactive power is related to the converter output current I_c and the voltage V_g. Based on the equivalent transformation equation given by Ref. [15], the maximum regulating capacity of Q_{DG} is:

$$Q_{\mathrm{c}} = \sqrt{\left(V_{\mathrm{g}} I_{\mathrm{c,max}}\right)^2 - P_{\mathrm{DG}}^2} \tag{4}$$

$$Q_{\mathrm{v}} = \sqrt{\left(\frac{V_{\mathrm{c,max}} V_{\mathrm{g}}}{X_{\mathrm{c}}}\right)^2 - P_{\mathrm{DG}}^2} - \frac{V_{\mathrm{g}}^2}{X_{\mathrm{c}}} \tag{5}$$

$$Q_{\mathrm{DG}} = \min\left\{Q_{\mathrm{c}}, Q_{\mathrm{v}}\right\} \tag{6}$$

Where $I_{\mathrm{c,max}}$ and $V_{\mathrm{c,max}}$ are respectively the maximum output current and the maximum voltage of the DG inverter side, whose calculation method can be seen in detail in Ref. [14]. Formula (4)-(6) show that when the DG active output and the power factor are certain, its reactive regulating range is also determined. In the decoupling condition above, DG reactive output can be controlled flexibly within established range, compared with conventional power factor control [11].

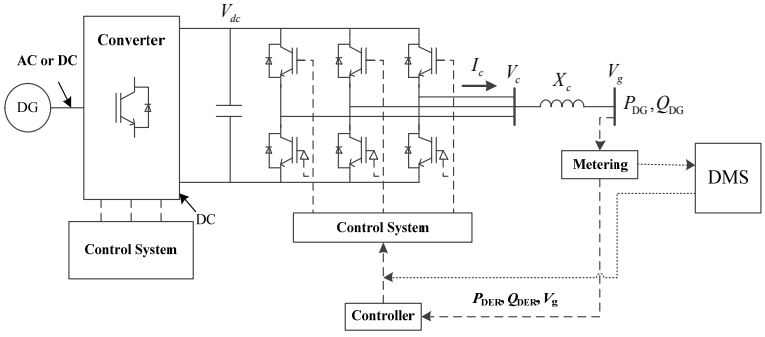

Figure 1 : Topology of DG based on DC/AC converter

ADN MULTI-OBJECTIVE OPTIMAL OPERATION MODEL

The conventional DG control strategy focusing on "local utilization" is hard to satisfy the need of ADN's large-scale use of renewable energy. With new topologies and advanced control technologies being applied under ADN, the degree of interconnection of the distribution network structure has been improved greatly so that the cross-regional usage of renewable energy has become a possibility.

Strategy for ADN operation considering cross-regional usage of renewable energy

Figure 2 shows an ADN system with cross-regional connection where DN1 and DN2 represent two power supply regions of the same voltage connected by tie lines. Assume DN1, as the study object, is a system with high permeability of DREG and DN2 is a passive distribution network which receives supply from higher grid and renewable energy from DN1. For the purpose of efficient utilization of renewable energy, we propose a strategy for ADN operation as follows:

The internal load demand of DN1 is supplied by upper grid, ESS, regional DREG and controllable DG: 1) When the output of DREG exceeds the load demand, extra power will charge the ESS first. After the devices are fully charged, the power will be sent to DN2 through tie line. If the transmission power reaches the upper limit of relevant devices, DREG will

have to cut its output or to quit operation. 2) When there is deficiency in the output of DREG, regional energy storage and upper grid will make up the difference in order. If requests are still not satisfied, controllable DG and ILs can be invoked to realize power balance.

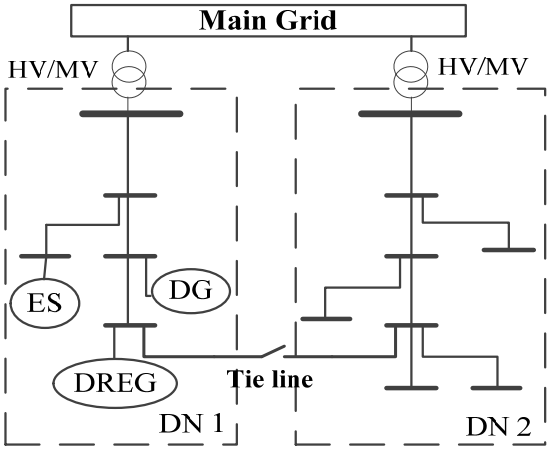

Figure 2 : ADN with cross-regional connection

For brevity, in the calculation of power flow, DN2 is set as equivalent virtual node *p'* whose scheduling mode and type of node come from the criterion in formula (7): 1) When formula (7) is satisfied, the renewable energy output of DN1 is surplus. Switch on the tie line and set *p'* as balance node and upper grid as PV node. 2) When formula (7) is not satisfied, the renewable energy output of DN1 is deficit. Switch off the tie line and set higher grid as balance bus.

$$\sum_{g\in\Omega_{\mathrm{DREG}}} P_g^{\mathrm{DREG}}(t) - \sum_{k\in\Omega_{\mathrm{D}}} P_k^{\mathrm{D}}(t) - \sum_{g'\in\Omega_{\mathrm{ESS}}} P_{g',\max}^{\mathrm{ESS+}}(t) - P^{\mathrm{it}}(t) > \varepsilon \tag{7}$$

Where Ω_{DREG}, Ω_{D} and Ω_{ESS} are the node sets of DREG, loads and energy storage devices; $P_g^{\mathrm{DREG}}(t)$, $P_k^{\mathrm{D}}(t)$, $P^{\mathrm{it}}(t)$ and $P_{g',\max}^{\mathrm{ESS+}}(t)$ are the output power of DREG, load demand, tie line transmission power and the maximum charging power of ESS during period *t*; ε is the discriminant margin.

For ensuring the direction of the power flow, Static Var Compensator (SVC) is assumed to have been installed at the tie line node of DN1. Besides, when applying this strategy, if the object ADN connects to multiple regional distribution networks, the grid with largest capacity on the tie line will be set as balance node.

Objective functions

We establish the optimization objectives of ADN day-ahead scheduling model respectively from three aspects: operation economic costs, utilization of renewable energy and power loss based on the ADN renewable energy control strategy listed above.

Objective function 1: minimum of the ADN operation economic costs

$$\min F_1 = \sum_{t=1}^{T}\left[C^{\mathrm{G}}(t) + C^{\mathrm{DG}}(t) + C^{\mathrm{ESS}}(t) + C^{\mathrm{IL}}(t)\right] \tag{8}$$

In the formula, $C^{\mathrm{G}}(t)$ is the power purchase costs generated in ADN during period *t*; $C^{\mathrm{DG}}(t)$ is the DG operation costs and $C^{\mathrm{ESS}}(t)$ is the energy storage operation costs during period *t*; $C^{\mathrm{IL}}(t)$ is the costs of applying the interruptible loads during period *t*; *T* is the period number that is corresponding to the scheduling period. The specific expansion of the formula above is notified as formula (9)-(12).

$$C^{\mathrm{G}}(t) = \lambda^{\mathrm{G}}(t) P^{\mathrm{G}}(t) \Delta t \tag{9}$$

$$C^{\mathrm{DG}}(t) = \sum_{g\in\Omega_{\mathrm{DG}}} \lambda_g^{\mathrm{DG}}(t) P_g^{\mathrm{DG}}(t) \Delta t \tag{10}$$

$$C^{\mathrm{ESS}}(t)=\sum_{g'\in\Omega_{\mathrm{ESS}}}\lambda^{\mathrm{ESS}}P_{g'}^{\mathrm{ESS}}(t)\Delta t \tag{11}$$

$$C^{\mathrm{IL}}(t)=\sum_{k'\in\Omega_{\mathrm{IL}}}[K_1(P_{k'}^{\mathrm{IL}}(t)\Delta t)^2+K_2(P_{k'}^{\mathrm{IL}}(t)\Delta t)-K_2(P_{k'}^{\mathrm{IL}}(t)\Delta t)\tau_{k'}] \tag{12}$$

In the formulas, $\lambda^{\mathrm{G}}(t)$ is the ADN power purchase price from the upper gird and $P^{\mathrm{G}}(t)$ is the injecting power during period t; Δt stands for the single dispatching interval (h); Ω_{DG} and Ω_{IL} respectively stand for the node sets of DG and interruptible loads in AND; $\lambda_g^{\mathrm{DG}}(t)$ is the DG grid purchase price at node g during period t; $P_g^{\mathrm{DG}}(t)$ is the DG generated energy at node g during period t; λ^{ESS} is the operation costs corresponding to the unit power provided by energy storage devices during period t; $P_{g'}^{\mathrm{ESS}}(t)$ is the charge/discharge power of the energy storage device at node g' during period t; K_1 and K_2 represent power shortage cost coefficients of interruptible loads; $P_{k'}^{\mathrm{IL}}(t)$ is the actual reduction quantity of the interruptible loads at node k' during period t; τ_{n} is a continuous variable in [0,1] that represents the interrupting will of the consumer's at node k'. The larger the value is, the higher the marginal power shortage cost and the expense of applying the IL [16].

Objective function 2: minimum of DREG power reduction quantity

$$\min F_2=\sum_{t=1}^{T}\sum_{g\in\Omega_{\mathrm{DREG}}}\left[\overline{P}_g^{\mathrm{DREG}}(t)-P_g^{\mathrm{DREG}}(t)\right]\Delta t \tag{13}$$

In the formula, $\overline{P}_g^{\mathrm{DREG}}(t)$ is the maximum calling power of DREG and $P_g^{\mathrm{DREG}}(t)$ is the actual power of DREG at node g during period t.

Objective function 3: minimum of system energy loss

In the framework of ADN, high permeability DG can change the inherent power flow of the distribution network and then influence the power loss. Therefore, the expression taking the minimum of system energy loss as the objective function can be written as:

$$\min F_3=\sum_{t=1}^{T}\sum_{ij\in\Omega_{\mathrm{F}}}Z_{ij}\left(P_{ij}^2+Q_{ij}^2\right)\Delta t\Big/U_j^2 \tag{14}$$

In the formula, Ω_{F} is the line gate set in the system; Z_{ij} is the resistance value of feeder line ij; P_{ij} is the active power through line ij and Q_{ij} is the reactive power; U_j is the end voltage of line ij.

Constrained conditions

The constrained conditions of the model mainly consist of network flow constraint and DREG characteristic constraint.

(a) Network flow constraint

Power balance constraint:

$$\begin{cases}P_i(t)=U_i(t)\sum_{j\in i}U_j(t)\left(G_{ij}\cos\theta_{ij}(t)+B_{ij}\sin\theta_{ij}(t)\right)\\ Q_i(t)=U_i(t)\sum_{j\in i}U_j(t)\left(G_{ij}\sin\theta_{ij}(t)-B_{ij}\cos\theta_{ij}(t)\right)\end{cases} \tag{15}$$

In the formula, $P_i(t)$ and $Q_i(t)$ are the active and reactive power input in node i during period t; $U_i(t)$ and $U_j(t)$ are the voltages at node i and its superior node j during period t; G_{ij} and B_{ij} are the conductance and susceptance of branch ij; $\theta_{ij}(t)$ is the phase difference between node i and j during period t.

Line current constraint:

$$I_{L,ij}(t) \le I_{L,ij,\max} \tag{16}$$

In the formula, $I_{L,ij}(t)$ is the current in branch *ij* during period *t*; $I_{L,ij,\max}$ is the maximum allowable current in branch *ij*.

Nodes voltage constraint:

$$V_{i,\min} \le V_i(t) \le V_{i,\max} \tag{17}$$

In the formula, $V_i(t)$ is the voltage at node *i* during period *t*; $V_{i,\min}$ and $V_{i,\max}$ are the minimum and maximum allowable voltages.

Balanced node constraint:

This model treats the upper grid and the regional tie line as positive and negative balance node. To restrain the influence on the outer system by the power fluctuation of ADN, we need to control the exchange power within a certain range, thus we have:

$$\begin{cases} P_{\min}^{\mathrm{gc}} \le P^{\mathrm{gc}}(t) \le P_{\max}^{\mathrm{gc}} \\ P_{\min}^{\mathrm{it}} \le P^{\mathrm{it}}(t) \le P_{\max}^{\mathrm{it}} \end{cases} \tag{18}$$

In the formula, $P^{\mathrm{gc}}(t)$ and P_{it}(t) are the active and reactive power in the higher grid during period *t*; $P_{\min}^{\mathrm{gc}}$, $P_{\max}^{\mathrm{gc}}$, $P_{\min}^{\mathrm{it}}$ and $P_{\max}^{\mathrm{it}}$ are the minimum and maximum allowable active power at the balance node.

(b) DER characteristic constraint

DG output constraint:

Restricted to technical characteristics and capacity constraint, the active and reactive adjustable output of DG needs to satisfy the following constraints:

$$\begin{cases} P_{\min,g}^{\mathrm{DG}} \le P_g^{\mathrm{DG}}(t) \le P_{\max,g}^{\mathrm{DG}} \\ Q_{\min,g}^{\mathrm{DG}} \le Q_g^{\mathrm{DG}}(t) \le Q_{\max,g}^{\mathrm{DG}} \\ \underline{PF}_g^{\mathrm{DG}} \le PF_{DG,g}(t) \le \overline{PF}_g^{\mathrm{DG}} \end{cases} \tag{19}$$

In the formula, $P_{\min,g}^{\mathrm{DG}}$ and $P_{\max,g}^{\mathrm{DG}}$ are the minimum and maximum active power supplied by DG at node *g* which are determined mainly by the supply of primary energy; $Q_{\min,g}^{\mathrm{DG}}$ and $Q_{\max,g}^{\mathrm{DG}}$ are the minimum and maximum of the adjustable reactive power supplied by DG under the decoupled state after the second section of calculation; $PF_{DG,g}(t)$ is the power factor of DG at node *i* during period *t*; $\underline{PF}_g^{\mathrm{DG}}$ and $\overline{PF}_g^{\mathrm{DG}}$ are the minimum and maximum of its allowable range.

Controlled DG ramp rate constraint:

To ensure the safe operation of controlled DG, we need to consider the following ramp rate constraint of the output power in multi-time intervals:

$$\begin{cases} P_g^{\mathrm{DG\_M}}(t) - P_g^{\mathrm{DG\_M}}(t-1) \le U_g \\ P_g^{\mathrm{DG\_M}}(t-1) - P_g^{\mathrm{DG\_M}}(t) \le D_g \end{cases} \tag{20}$$

In the formula, $P_g^{\mathrm{DG\_M}}(t)$ and $P_g^{\mathrm{DG\_M}}(t-1)$ are the active output power supplied by the controlled DG at node *g* during period *t* and *t-1*; U_i and D_i are the maximum of its uplink and downlink rate of change.

Energy storage device scheduling constraint:

The operation of ESS needs to simultaneously satisfy charge/discharge state constraint, charge/discharge power constraint and charged state constraint [17]:

$$P_{g'}^{\mathrm{ESS}+}(t)\square P_{g'}^{\mathrm{ESS}-}(t)=0 \tag{21}$$

$$\begin{cases}-P_{g',\mathrm{rated}}^{\mathrm{ESS}+}<P_{g'}^{\mathrm{ESS}+}(t)<0\\0<P_{g'}^{\mathrm{ESS}-}(t)<\varepsilon_{\mathrm{out}}P_{g',\mathrm{rated}}^{\mathrm{ESS}+}\end{cases} \tag{22}$$

$$\mathrm{SOC}_{\min,g'}^{\mathrm{ESS}}<\mathrm{SOC}_{\min,g'}^{\mathrm{ESS}}(t)<\mathrm{SOC}_{\max,g'}^{\mathrm{ESS}} \tag{23}$$

In the formulas, $P_{g'}^{\mathrm{ESS}+}(t)$ and $P_{g'}^{\mathrm{ESS}-}(t)$ are the charge/discharge power of the energy storage device at node *g'* during period *t*; $P_{g',\mathrm{rated}}^{\mathrm{ESS}+}$ is the rated charging power of the energy storage device at node *g'*; $\mathrm{SOC}_{\max,g'}^{\mathrm{ESS}}$ and $\mathrm{SOC}_{\min,g'}^{\mathrm{ESS}}$ are the maximum and minimum capacity of the energy storage device at node *g'*. After a whole scheduling cycle, the charged state of the energy storage device should be the same as before scheduling, thus we have:

$$\mathrm{SOC}_{g'}^{\mathrm{ESS}}(t_0)=\mathrm{SOC}_{g'}^{\mathrm{ESS}}(t_n) \tag{24}$$

Interruptible load tapping constraint:

In ADN, the tap of interruptible loads is confined by available capacity, break lasting time, time interval and tapping times, etc. [18]. Thus the following constrains should be satisfied:

$$P_{\min,k'}^{\mathrm{IL}}\le P_{k'}^{\mathrm{IL}}(t)\le P_{\max,k'}^{\mathrm{IL}} \tag{25}$$

$$\Delta D_{\min,k'}^{\mathrm{IL}}\le(t''|_{J_{\mathrm{off},k'}=1}-t'|_{J_{\mathrm{on},k'}=1})\le\Delta D_{\max,k'}^{\mathrm{IL}} \tag{26}$$

$$(t''|_{J_{on,k'}=1}-t'|_{J_{\mathrm{on},k'}=1})\ge\Delta IV_{\min,k'}^{\mathrm{IL}} \tag{27}$$

$$0\le\sum_{t=1}^{T}J_{on,k',t}\le\varpi_{\max,k'}^{\mathrm{IL}} \tag{28}$$

In the formulas, $P_{\min,k'}^{\mathrm{IL}}$ and $P_{\max,k'}^{\mathrm{IL}}$ are the minimum and maximum interruptible power at node *k'*; $J_{\mathrm{on},k'}$ and $J_{\mathrm{off},k'}$ represent the tapping and de-tapping pointers of the interruptible load at node *k'*. When the load is interrupted, $J_{\mathrm{on},k'}$, corresponding to the starting time, is set to 1, else it is 0; when the load is recharged, $J_{\mathrm{off},k'}$, corresponding to the recovering time, is set to 1, else it is 0. Besides, $J_{\mathrm{off},k'}$ and $\Delta D_{\max,k'}^{\mathrm{IL}}$ are the minimum and maximum supply break lasting time limit of the load at node *k'*; $\Delta IV_{\min,k'}^{\mathrm{IL}}$ is the minimum time interval between two supply breaks that users at node *k'* can tolerate; $\varpi_{\max,k'}^{\mathrm{IL}}$ is the maximum tapping times of the interruptible load at node *k'* in an operational cycle.

SOLUTION METHOD

The model proposed is a complex high-dimensional multi-objective nonlinear optimization problem. For this case harmony Search (HS) algorithm is a novel intelligent optimization algorithm proposed by Geem Z.W et al. in 2001. Its basic theory is to realize optimization by imitating the methods which composers use repeatedly to find the most suitable tune. HS has powerful capability of global search and fast convergence rate, compared with conventional intelligent optimization algorithms such as genetic algorithm and particle swarm algorithm [19]. Several improvements are made by Refs. [20] and [21] to enhance the HS's ability of global search while ensuring its rate of convergence, so that it was adjusted to multi-objective optimization problems.

This paper applies MOHS algorithm, which is based on the crossover strategy, to solve the model. The calculation procedure is showed in Figure 3.

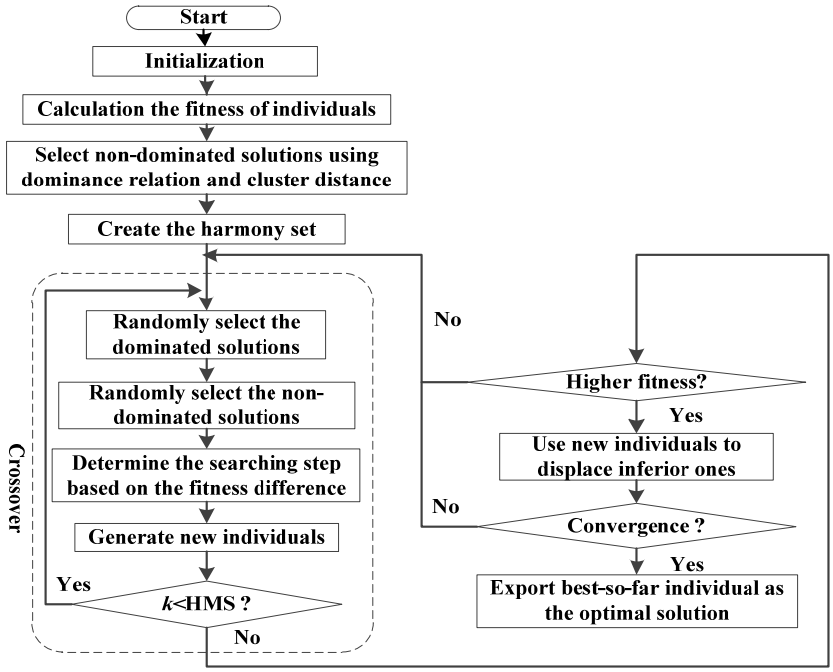

Figure 3 : Optimization procedures based on MOHS

The explanations for the critical process are as follows:

- Algorithm parameters initialization: The MOHS computing parameters that need to be initialized include the Harmony Memory Size (HMS), the Harmony Memory Consideration Rate (HMCR) and maximum iterations K_{max}.
- Dominated ranking: The multi-objective optimization problem can be defined as formula (29) where the decision vector $X=(x_1,x_2,\ldots,x_n)^H$ belongs to feasible region H.

$$\begin{aligned}&\min\{f_1(X),f_2(X),\ldots,f_m(X)\}\\&X\in H\end{aligned} \tag{11}$$

The dominance relations of each harmony in the harmony memory are computed. When decision vectors X_1 and X_2 meet formulation (30), X_2 is dominated by X_1.

$$\begin{cases}\forall i: f_i(X_1)\le f_i(X_2), i=1,\ldots,m\\ \exists i\,|\, f_i(X_1)<f_i(X_2), i=1,\ldots,m\end{cases} \tag{12}$$

Compute the dominated amount of the overall harmonies in sequence. Select and shift the non-dominated solutions into harmony memory pool. Grade and sequence the dominated solutions based on the dominated amount.

- Crowding distance: As for the harmonies in the same grade, the method in Ref. [22] is applied to compute the crowding distance of each harmony and sequence of the harmonies in the same rank based on the congestion degree.
- Crossover strategy: In the intelligent optimization algorithm, the diversity of the solution set declines with the increase of the iterations. Besides, increasing the diversity of the solution set will decrease the convergence rate of the algorithm. This paper utilizes the crossover strategy to optimize the algorithm performance. The new harmony generating algorithm can be written as (31) [20]:

$$X^{\text{new}}=X^{\text{Nd}}\pm\text{rand}\times\left|X^{\text{Nd}}-X^{\text{d}}\right| \tag{13}$$

In the formula, X^{new} is the new harmony; X^{Nd} and X^{d} are the non-dominated and dominated harmonies selected randomly from the harmony memory; rand is the random number generated via HMCR.

CASE STUDY

Basic data

To verify the effectiveness of the proposed model, this paper takes an expanded 33-bus distribution system [23] as a case study（Figure 4）. The DREG information in the system is as follows: photovoltaic∈{7,13,32}, capacity for each node is 1 MW; wind turbine∈{21,27}, capacity for each node is 0.8 MW; micro gas turbine∈{24,30}, power range is 0.1 MW~0.4 MW; ESS∈{6,29}, upper limit of total in/out power of each node is 0.24 MW, capacity is 1.2 MWh, SOC range is 30%~90%, charging efficiency is 80%. The ILs are adjusted by the feed breaker and controlled by a constant power factor, and each manageable node load is shown in TABLE 1. We assume each node load is kept off at once within 24 hours mostly, and each break off lasts less than 2 hours.

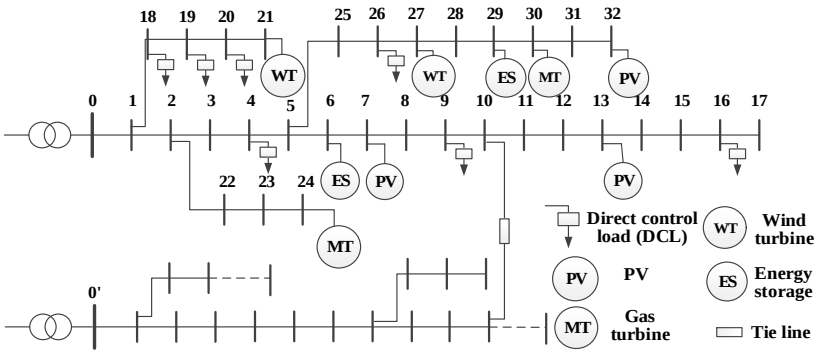

Figure 4 : Modified 33-node distribution system

TABLE 1 : Capacity of interruptible loads at different buses

Node number	Controlled power (kVA)
4	42+j21
9	30+j10
16	48+j16
18	45+j20
19	45+j20
20	72+j32
26	36+j15

The load curve of the system during the day is cited from Ref. [24], while the illumination and wind speed data are adopted from an actual research. Based on standard, the tariffs of photovoltaic and wind power are 1 Yuan/kWh and 0.8 Yuan/kWh; the tariff of micro gas turbine is 0.81 Yuan/kWh; the electricity price from the upper grid is 0.38 Yuan/kWh; the cost coefficients of interruptible load [18] K_1 and K_2 are 5000 and 3200 respectively. We assume that the deviation range of the node voltage is ±5%.

The algorithm parameters are: HMS=40; K_{max}=500; adjusting HMCR based on dynamic strategy, $HMCR_{max}$=0.9, $HMCR_{min}$=0.6.

Optimal result analysis

(a) Pareto optimal solution analysis

The calculated Pareto front is shown in Figure 5 where DREG is controlled under power factor 0.9. The Pareto solution set solved by MOHS is well distributed, and is able to provide a wealth of information to the balance among economic cost, network loss and utilization of renewable energy. Based on the Pareto result above, an optimized operational plan could be achieved through the expectations and requirements of the ADN operators.

From Figure 5, it can be seen that to achieve the cross-regional consumption of renewable energy, the power loss will increase with the transmission distance extending. Meanwhile, to deal with the fluctuation of DREG, we have to take advantage of resources such as micro gas turbines, ESS and ILs more frequently, which further increases the total cost of the system. Based on the Pareto optimized result above, in actual applications we can base on the specific expectations and requirements of the ADN operator and finally determine a systematic scheduling operation plan scientifically.

(b) Power balance analysis

In order to clearly reveal the daytime output and energy constitution of ADN, we pick out two cases from the former section when the curtailment of DREG are 5% and 15%, and power balance is analyzed to the optimized operation plan. The operation points of each DG and ESS as well as the switching conditions of interruptible loads are shown in Figure 6.

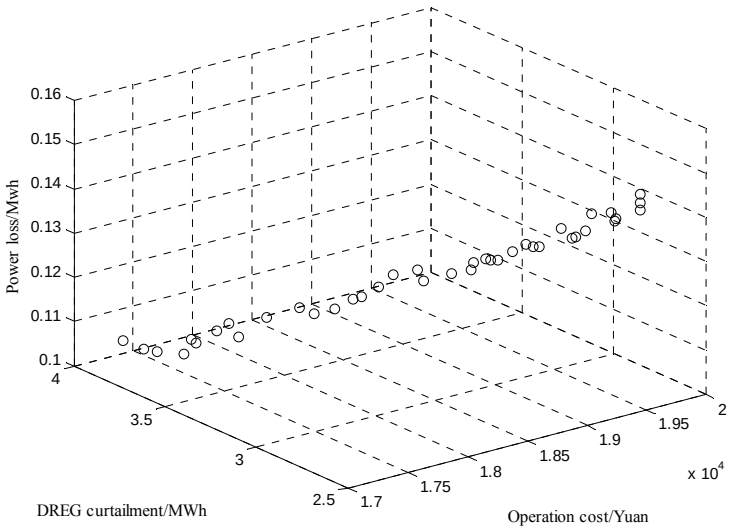

Figure 5 : Pareto fronts between different objectives

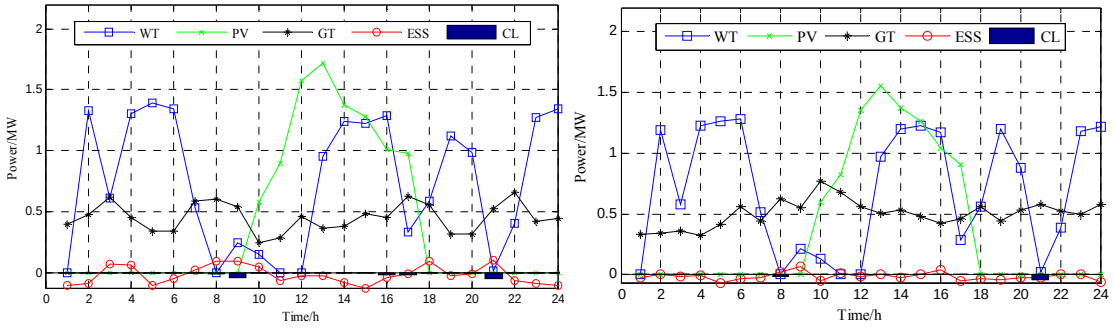

A. DREG power extraction=5% **B. DREG power extraction=15%**

Figure 6 : Optimal scheduling plan of AND

The results indicate that it is sensitive to outside factors under DREG of high permeability. Meanwhile, the utilization of ESS and demand side resources enhances the utilization of renewable energy.

(c) Cross-regional consumption strategic analysis

To verify the influence of the cross-regional consumption strategy on the utilization of renewable energy, a comparison is made to analysis the optimal operational plans under different situations. Case 1 considers the cross-regional consumption strategy and Case 2 merely considers local consumption. After optimal calculation, the resulted Pareto fronts under each situation are shown in Figure 7, while TABLE 2 gives the cases of eclectic optimal solution.

By calculation, the daily utilization ratio of renewable energy under Case 1 and 2 are 88.2% and 85.1% respectively. Thus it is clear that the cross-regional consumption strategy promotes the increase of the utilization efficiency of DREG (i.e. decrease of DREG power curtailment). Meanwhile, TABLE 2 shows that the implementation of the cross-regional consumption strategy increases the network loss. This indicates that due to the connection between systems, the transmission range of the DG output energy in ADN is extended, and therefore the power loss also gradually increases. Besides, with the decrease of DREG output, the frequency and depth of ESS and controllable loads increase, and therefore lower the operation cost of ADN.

If the contact distribution network is regarded as the receiving balance node, the maximum transmission power of the tie line is set as the upper capacity. When the power exceeds the upper limit, the output of DREG is decreased to ensure the stability of the system.

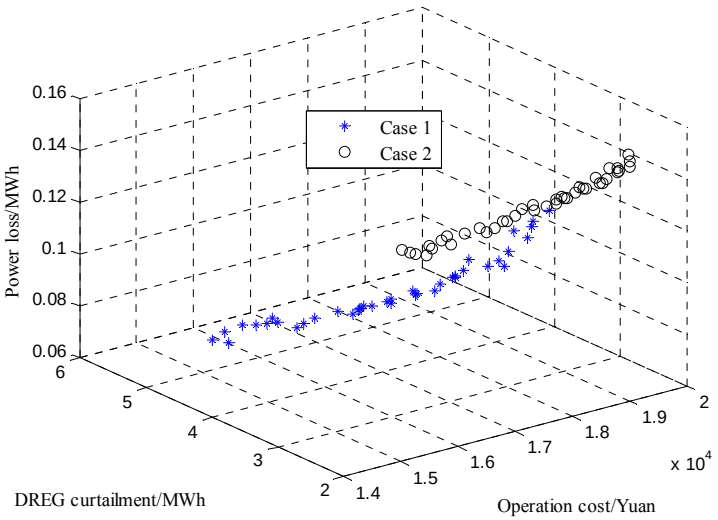

Figure 7 : Pareto fronts under different cases

TABLE 2 : Objective function values for different cases

	Operation cost (¥*10^4 yuan)	DREG curtailment (MWh)	Energy loss (MWh)
Case-1	1.87	3.83	0.12
Case-2	1.68	4.89	0.09

(d) DREG active and reactive decoupling control analysis

Based on formula (4)-(6), different power factors correspond to different reactive adjustment ability of DREG: 1) when pf=1, DREG has no reactive adjustment ability, in this case the utilization ratio of DREG is 86.7%. 2) when pf=0.9, DREG has adjustment ability, but it has to sacrifice some active output for reactive adjustment, and the utilization ratio of DREG is 88.2%. 3) when pf=0.8, the reactive adjustment ability of DG further increases, and the active output keeps decreasing, and the utilization ratio of DREG is 78.9%.

By comparison it is known that if we consider the reactive adjustment ability of DREG, the system power flow distribution and voltage quality can be improved significantly, so as to promote the consumption efficiency of the whole system. Considering the operational cost, (pf=0.9)>(pf=1)>(pf=0.8), which indicates that the decrease of utilization of DREG leads to lower percentage of renewable energy in the system energy constitution. And since $C_{DREG}>C_{gsp}$, the operation cost decreases.

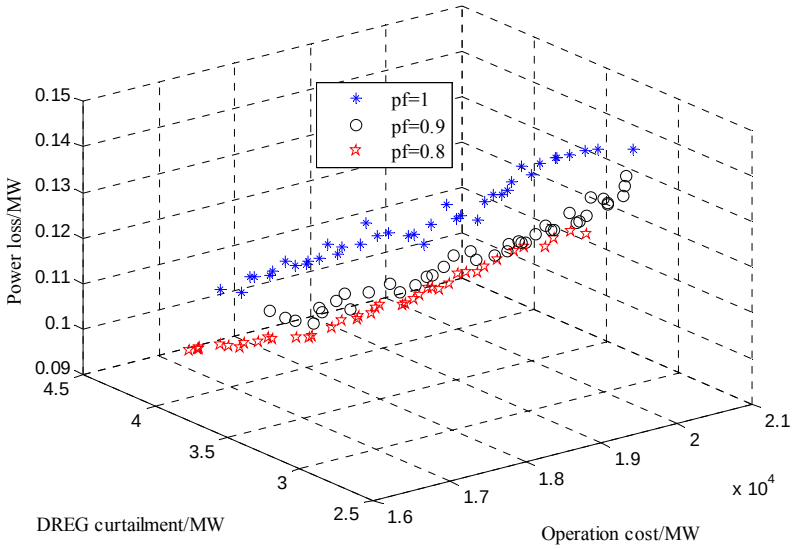

Figure 8 : Pareto fronts for different power factors of DREG

TABLE 3 : Objective function values under different power factors of DREG

	Operating cost (¥ *10^4 yuan)	DREG curtailment(MWh)	Energy loss (MWh)	DREG power factor (%)
pf=1	1.79	4.36	0.13	86.7
pf=0.9	1.87	3.84	0.12	88.2
pf=0.8	1.66	6.95	0.09	78.9

All in all, when the reactive adjustment ability of DREG is taken into account, although the overall operation efficiency of ADN and the electricity quality can be improved, the active output of DREG decreases by a lower power factor. Therefore the optimal power factor of DREG should be determined by sensitivity analysis based on the permeability of renewable energy in the system.

CONCLUSION

For the purpose of achieving high efficiency of renewable energy usage, this paper proposes a multi-objective optimization method for ADN operation. The DG active/reactive power decoupling control ability under the inverter-based interface mode is analyzed and an ADN cross-regional energy absorptive strategy is put forward. On this basis, an ADN multi-objective optimization dispatching model aiming at the minimum of system operation cost, DREG contribution curtailment and the power loss is established. The model is solved by MOHS algorithm. Conclusions can be reached with the analysis of an expanded 33-bus distribution system:

I. In ADN, the efficiency of DREG, economic costs and the power loss interplay. The increase of the DREG utilization rate raises the system operation cost and the overall network loss indirectly.

II. The cross-regional energy absorptive strategy is in favor of the efficient utilization of renewable energy. The system operation loss also increases to certain extent with the enlargement of the transmission range of DREG output energy.

III. Although considering the DREG reactive power regulating ability will restrict its active contribution, it could also improve the system power flow distribution and the energy quality at the DG nodes, so it still has significant positive effect on improving the utilization of renewable energy and the efficiency of system overall operation.

In conclusion, the optimizing model proposed in the paper could realize comprehensive benefit optimization of ADN operation on the premise of prior utilization of renewable energy. It is able to meet different needs of multiple system operators and relevant results can offer theoretical foundation and experience to the formulation of ADN operation dispatching strategy.

REFERENCES

[1] (CIGRE) Development and Operation of Active Distribution Network. Report no.978-2-85873-146-9 (2011).

[2] L. F. Ochoa, G. P. Harrison. Minimizing energy losses: optimal accommodation and smart operation of renewable distributed generation. IEEE Transactions on Power Systems, 26 1 (2012).

[3] J. Zhang, B. Zeng, Y. Zhang, et al. Key Issues and Research Prospects of Active Distribution Network Planning. Transactions of China Electrotechnical Society, 2 29 (2014).

[4] T. Adrian, L. Mats, Y. Cherry. Active management of distributed energy resources using standardized communications and modern information technologies. IEEE Transactions on Industrial Electronics, 56 10 (2009).

[5] P. Fabrizio, P. Giuditta, G. S. Gian. Optimal coordination of energy resources with a two-stage online management. IEEE Transactions on Industrial Electronics, 58 10 (2011).

[6] M. J. Dolan, E. M. Davidson, I. Kockar, et al. Distribution power flow management utilizing an online optimal power flow technique. IEEE Transactions on Power Systems, 27 2 (2012).

[7] A. Borghetti, M. Bosetti, S. Grillo, et al. Short-term scheduling and control of active distribution system with high penetration of renewable resources. IEEE Journal on Systems, 4 3 (2010).

[8] Y. You, D. Liu, Q. Zhong, et al. Research on optimal schedule strategy for active distribution network. Automation of Electric Power Systems, 3 89 (2014).

[9] S. Gill, I. Kockar, W. Ault. Dynamic optimal power flow for active distribution networks. IEEE Transactions on Power Systems. 29 1 (2014).

[10] J. Wang, H. Xie, J. Sun. Study on energy dispatch strategy of active distribution network using chance-constrained programming. Power System Protection and Control, 42 13 (2014).

[11] Y. You, D. Liu, Q. Zhong, et al. Multi-time scale coordinated control of distributed generators based on active distribution network. Automation of Electric Power Systems, 38 9 (2014).

[12] Y. Liu, W. Wu, B. Zhang, et al. A mixed integer second-order cone programming based active and reactive power coordinated multi-period optimization for active distribution network. Proceedings of the CSEE, 34 16 (2014).

[13] R. U. Nayeem, B. Kankar, T. Torbjorn. Wind farms as reactive power ancillary service providers— technical and economic issues. IEEE Transactions on Energy Conversion, 24 3 (2009).

[14] C. R. Augusto, P. Antonio. Distributed generators as providers of reactive power support—a market approach. IEEE Transactions on Power Systems, 28 1 (2013).
[15] C. Vito, C. Gaspare, G. Vincenzo, M. Giovanni, et al. Optimal Decentralized Voltage Control for Distribution Systems With Inverter-Based Distributed Generators. IEEE Transactions on Power Systems, 29 1 (2014).
[16] B. Zeng, J. Dong, J. Zhang. A coordinated planning approach for grid-side integrated resources in an energy-saving service environment. Automation of Electric Power Systems, 3 19 (2013).
[17] G. Aouss, L. Pu. Active-reactive optimal power flow in distribution networks with embedded generation and battery storage. IEEE Transactions on Power Systems, 27 4 (2012).
[18] K. Hyung-Geun, K. Jin-O, Optimal combined scheduling of generation and demand response with demand resource constraints. Applied Energy, 96 (2012).
[19] Z. W. Geem, J. H. Kim, Loganathan G V. A new heuristic optimization algorithm: harmony search, Simulation, 76 (2011).
[20] D. X. Zou, L. Q. Gao, J. H. Wu, et al. A novel global harmony search algorithm for reliability problems. Computers & Industrial Engineering, 58 (2010).
[21] N. Komail, M. F. Malihe, N. Hossein, et al. An improved multi-objective harmony search for optimal placement of DGs in distribution systems. IEEE Transactions on Smart Grid, 4 1 (2013)
[22] C. Peng, H. Sun. Multi-objective optimization power dispatch based on non-dominated sorting differential evolution. Proceedings of the CSEE, 29 34 (2009).
[23] M. E. Baran, F. F. Wu. Network reconfiguration in distribution systems for loss reduction and load balancing. IEEE Transactions Power Delivery, 4 2 (1989).
[24] B. Zeng, J. H. Zhang, X. Yang, et al. Integrated planning for transition to low-carbon distribution system with renewable energy generation and demand response. IEEE Transactions on Power Systems, 29 3 (2014).